Mokslas – Lietuvos ateitis / Science – Future of Lithuania
ISSN 2029-2341 / eISSN 2029-2252
2018 Volume 10, Article ID: mla.2018.4093, 1–9
https://doi.org/10.3846/mla.2018.4093

Transport engineering and management
Transporto inžinerija ir vadyba

RME CO-COMBUSTION WITH HYDROGEN IN COMPRESSION IGNITION ENGINE: PERFORMANCE, EFFICIENCY AND EMISSIONS

Alfredas RIMKUS, Romualdas JUKNELEVIČIUS *

Vilnius Gediminas Technical University, Vilnius, Lithuania

Received 22 July 2018; accepted 24 October 2018

Abstract. The article presents the test results of the single cylinder CI engine with common rail injection system operating on biofuel – Rapeseed Methyl Ester with addition supply of hydrogen. The purpose of this investigation was to examine the influence of the hydrogen addition to the biofuel on combustion phases, engine performance, efficiency, and exhaust emissions. HES was changed within the range from 0 to 44%. Hydrogen was injected into the intake manifold, where it created homogeneous mixture with air. Tests were performed at both fixed and optimal injection timings at low, medium and nominal engine load. After analysis of the engine bench tests and simulation with AVL BOOST software, it was observed that lean hydrogen – RME mixture does not support the flame propagation and efficient combustion. While at the rich fuel mixture and with increasing hydrogen fraction, the combustion intensity concentrate at the beginning of the combustion process and shortened the ignition delay phase. AVL BOOST simulation performed within the wide range of HES (16–80%) revealed that combustion intensity moves to the beginning of combustion with increase of HES. Decrease of CO, CO_2 and smoke opacity was observed with increase of hydrogen amounts to the engine. However, increase of the NO concentration in the engine exhaust gases was observed.

Keywords: hydrogen, RME, diesel fuel, CI engine, combustion, emission, abnormal combustion.

Introduction

The recent revolutions in Arab countries, continuous civil wars in the North Africa and Middle East, Iran nuclear crisis, sanctions of US on Russia make concerns about the stability of the energy sources and force the industry to look for sustainable energy sources supplied by reliable domestic suppliers and thus avoid the costly delivery. The tide relation between oil production and global growth of economy (Murray & King, 2012) or in other words the impact of oil to the economy, and location of the reserves in the certain regions of the World, implicates the research of alternative energy resources.

There are few routes to ease the burden of road transport emissions, to add renewable fuel to the fossil fuel or, substitute the fossil fuel with renewable fuel. The use of renewable fuels has the potential to reduce the emissions and, thus mitigate the effects of the environmental crisis of climate change. Among the current renewable fuels are alternative biomass based biofuels.

The physical properties and the availability in the globe makes the hydrogen the other quite attractive alternative fuel for road transport. Verhelst and Wallner (2009), Barreto, Makihira, and Riahi (2003), described the long-term scenario of hydrogen usage as an energy source including it qualitative and quantitative descriptions in order to implement the transition towards clean and sustainable energy. The authors demonstrated the importance of variety of hydrogen-based energy technologies, which enable the efficient and economical way to ensure energy needs.

Although the use of sole hydrogen for combustion engines are hardly possible, the co-combustion with various fuels including renewable fuels makes it the subject of research interest. Moreover, it is widely known, that there is no single fuel solution for the future transport because the availability and cost of alternative fuels differ between the modes. The discussion in this study will be focused on the co-combustion of hydrogen with RME.

The current alternative biomass based biofuels are lumped into first, second and third-generation categories and their use may improve the emissions levels. The first generation refers to biofuels produced from commonly available, edible feedstock's using well-established conversion technologies (Hoekman, Broch, Robbins, Ceniceros, & Natarajan, 2012; Silvestrini et al., 2010; Raslavičius,

*Corresponding author. E-mail: *romualdas.juknelevicius@vgtu.lt*

Keršys, Starevičius, Sapragonas, & Bazaras, 2014; Murphy & Hall, 2010; Hilbers et al., 2015). Most biofuels today are classified as first-generation and they can offer some CO_2 benefits and can help improve domestic energy security (Silvestrini et al., 2010; Raslavičius et al., 2014). Biofuels produced from second-generation biomass does not compete with food production. High raw material costs and energy return on energy invested are main issues in making biofuel processes economically attractive (Murphy & Hall, 2010).

The main sources of biofuels are fatty acids of vegetable oils and animal fats. Vegetable oils consist of a mixture of triglycerides, i.e. esters of glycerol and unsaturated fatty acids. Transesterification of triglycerides with methanol gives a mixture of FAME and glycerol, which can be also considered as engine fuel (Grab-Rogalinski & Szwaja, 2016). The transesterification of rapeseed oil containing the triglyceride ($C_3H_5(C_{18}H_{31}O_2)_3$), involves it reaction with alcohol (CH_3OH) in presence of a catalyst ($NaOH$). The final products of this reaction are glycerol ($C_3H_5(OH)_3$) and RME ($C_{17}H_{31}COOCH_3$) (Knothe, Gerpen, & Krahl, 2005; Jučas, 2006):

$$C_3H_5(C_{18}H_{31}O_2)_3 + NaOH + 3CH_3OH \rightarrow C_3H_5(OH)_3 + 3C_{17}H_{31}COOCH_3. \quad (1)$$

FAME is usually referred to as conventional biodiesel (Murphy & Hall, 2010). FAME can be produced of any triglyceride feedstock, including oil-bearing crops, animal fats, and algal lipids. Most of biofuel properties correlate directly with the fatty acid profile, and thus the source feedstock (Knothe & Razon, 2017). The properties of the RME along with petroleum diesel and hydrogen presented at the Table 1.

Subsequent studies (Zhou, Cheung, & Leung, 2014; Baltacioglu, Arat, Ozcanli, & Aydin, 2016; Senthil Kumar, 2003; Singh Bika, Franklin, & Kittelson, 2008) of the CI engine with different amount of hydrogen addition show that emissions and performance parameters are dependent on injection timing of diesel fuel, it's duration, *BMEP*, *MFB* and engine speed. Tests carried out with a CI engine operated with hydrogen – diesel mixture (Hilbers et al., 2015) with amount of hydrogen energy share of 15% p_{max} increased, with hydrogen share of 17%, combustion knock appeared, with hydrogen share of 25%, the peak of the MFB rate increased and generated even higher combustion knock.

Experiments carried out on the CI engine (Aldhaidhawi, Chiriac, Bădescu, Descombes, & Podevin, 2017) with fossil DF blended with 20 vol% of RME and HES of 0–5%, revealed the lower engine performance, efficiency, and emissions except the NO_x, which slightly increased. Addition of hydrogen to the fuel blend, the CO emissions, smoke, and THC decreased.

Tests carried out with amounts of HES = 5% (Szwaja & Grab-Rogalinski, 2009) fossil DF, shortens the CI engine ignition lag and, decrease the rate of pressure rise. With HES of 17%, the combustion knock starts and with HES of 25%, the fast combustion accompanied by combustion knock.

Rimkus, Žaglinskis, Rapalis, and Skačkauskas (2015) performed tests of CI engine operating on biomass-to-liquid – diesel blend, and revealed that NO_x increased while the positive effect on efficiency and emissions was defined. Therefore further research is needed to find ways to reduce increased NO_x whilst maintain the efficiency. Tests carried out using RME with addition of 3 l/min hydrooxile gas examined the impact of low hydrogen amounts on engine performance (Rimkus, Matijošius, Bogdevičius, Bereczky, & Török, 2018). HHO gas reduced the maximum brake torque by 2.6–2.7%, at engine speeds of 1900–3700 rpm, CO_2 increasd by 6% and NO_x by 10%. CO_2 increased because the HHO containing hydrogen and oxygen improve the carbon oxidation, while NO_x increased due to increased combustion temperature.

These reviewed experiments either performed on of the CI engine, with sole biodiesel or with addition of hydrogen to the fossil DF or FAME fuel blends. There are some gaps in knowledge dealing with hydrogen-assisted

Table 1. Fuel properties (Rapsoila Certificate of Analysis No. 03/17, 2017; Labeckas, Slavinskas, & Mažeika, 2014; Hoekman et al., 2012; Verhelst & Wallner, 2009)

Properties	Petroleum Diesel	RME	Hydrogen
Chemical formula	$C_{10}H_{22} - C_{15}H_{32}$	$C_{17}H_{31}COOCH_3$	H_2
Composition, %wt	84–87 C, 13–16 H	77.5–77.9 C, 11.3–11.7 H, 10.8 O_2	100
Density, kg/m³ at 15°C and 1.01 bar	835.3	883.7	0.08985
Lower heating value, MJ/kg	42.5	37.4	120
Lower heating value, MJ/Nm³	36350	32700	10.7
Stoichiometric air-fuel ratio, kg/kg	14.5	12.4	34.2
Heating value of stoichiometric mixture, MJ/kg	2.74	2.79	3.40
Heating value of stoichiometric mixture, MJ/Nm³	3.60	3.58	3.00
Auto ignition temperature at STP,°C	250	342	585
Flammability limits at NTP, %vol	0.6–7.5	0.8–10	4–75
Cetane number	54.6	51.7	5–10
Carbon to hydrogen ratio (C/H)	6.9	6.5	–

combustion of pure biofuels in the CI engine. The purpose of this research is to conduct the analysis of the effect of neat hydrogen co-combustion with RME on the performance and emissions parameters of a CI engine operating at a Low, Medium, Nominal Loads and with fixed start of DF injection. The objectives of this research may be stated as follows:

- Determine the effect of hydrogen fraction on co-combustion with RME on the in-cylinder pressure, *ISFC*, *ITE* when running with HES form 0% to 44% and at various loads,
- Evaluate the effect of HES on co-combustion with RME on the changes of emissions, including the NO, CO, CO_2 and smokiness,
- Determine the influence on combustion duration and intensity of hydrogen co-combustion with RME at various loads by using AVL BOOST simulation with HES form 0% to 80%.

Addition of the sufficient hydrogen fraction with high LHV shortens the CI engine ignition lag, increase the efficiency and performance of the engine until the combustion knock appeared and increased NO_x. The tests performed during this research at the broad range of loads and HES at the fixed injection timing of RME, enable to compare engine parameters at various HES and to determine the favourable outcome of hydrogen addition as it is limited by combustion knock.

1. Experimental set-up and procedure

Tests have been performed at the Institute of Thermal Machinery of Czestochowa University of Technology, in Poland. The single cylinder water cooling stationary CI engine Andoria S320 equipped with high pressure Bosch common rail fuel pump driven by an electric motor. The installation of the test bed shown at the Figure 1.

Displacement of the engine – 1810 cm^3, compression ratio – 17. After CI engine starts to run, it delivers energy by driving belts to generator. The engine was set to operate at the constant speed of 965 rpm ± 0.83%.

The *IMEP* was managed by changing the liquid and gaseous fuel (H_2) supply to the combustion chamber. The hydrogen was supplied together with air into the intake manifold. In cylinder, air – hydrogen mixture under the elevated heat and pressure self-ignited by injected diesel fuel.

Pollutants in the exhaust gas were analyzed using *Bosch* and *Maha* (smoke) analyzers. In-cylinder pressure (*p)* fixed by piezo sensor *Kistler* 6061B installed instead of the preheating plug. The crank angle (CA) fixed by encoder *Kistler* type 2612C. The data acquisition converter *Measurement Computing Corporation* PCI-DAS 6036 was used in line with PC software *SAWIR* – System of the Indicator Chart on Real Time Analysis. Tests of the RME were performed under the LL of *IMEP* = 262.5–295.6 kPa, ML of *IMEP* = 379.7–508.5 kPa and NL of *IMEP* = 519.2–625.3 kPa. As the presence of hydrogen effects the combustion duration, the start of diesel injection timing φ,

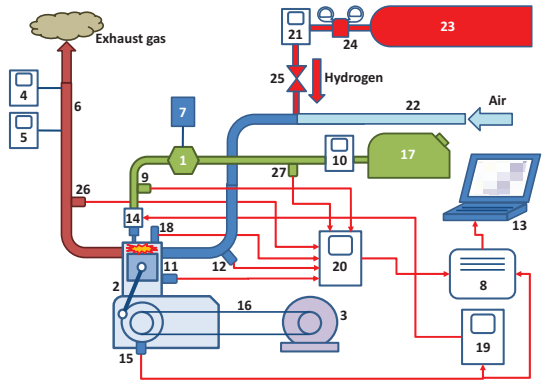

Figure 1. Experimental installation.
1 – DF pump, 2 – CI engine, 3 – Generator, 4 – Smoke analyser, 5 – Emission analyser, 6 – Exhaust pipe, 7 – DF pump drive el. engine, 8 – Data acquisition system, 9 – DF pressure sensor, 10 – DF flow meter, 11 – Engine temperature sensor, 12 – Inlet air temp. sensor, 13 – PC – SAWIR, 14 – DF common rail injector, 15 – CA encoder, 16 – Drive belt, 17 – DF tank, 18 – In-cylinder pressure sensor, 19 – DF injection controller, 20 – Amplifiers & A/D converters, 21 – Hydrogen flow meter, 22 – Air intake pipe, 23 – Hydrogen balloon, 24 – Hydrogen one-stage pressure regulator, 25 – Hydrogen firebreak arrestor, 26 – Exhaust gas temperature sensor, 27 – DF temperature sensor

during tests of hydrogen – biofuel mixture was set at the fixed position, enabling to compare and analyze engine parameters at various HES.

The injection timing φ_1 for RME operation (Table 2, test no. 1) was determined at the position of 50% MFB, which corresponds to the peak of indicative pressure in cylinder. This position was set within the range of 10–15 CAD ATDC. Other injection timing φ_2 (Table 2, test no. 2) was determined with the lowest HES, again at the combustion of 50% MFB within the range of 10–15 CAD ATDC. And the same injection timing φ_2 was used for the rest of HES: 26%, 32%, 39%, 44%. At the ML operation φ_1 = 22 deg (Table 2, test no. 3) was determined at the HES = 0%, and injection timing was fixed at φ_2 = 20 deg with change of the HES as following: 16%, 23%, 30%, 37%, 42%. At the NL operation φ_1 = 28 deg was determined at the HES = 0%, and φ_2 = 26 deg was fixed with change of the HES as following: 16%, 23%, 30%, 36%.

Table 2. Injection timing and IMEP at various compositions of combustible mixture.

Test no.	Composition of combustible mixture	φ, BTDC	Loads
1	RME+H_2 0%	φ_1 = 16°	LL
2	RME+H_2 (19–44%)	φ_2 = 14°	LL
3	RME+H_2 0%	22°	ML
4	RME+H_2 (16–42%)	20°	ML
5	RME+H_2 0%	28°	NL
6	RME+H_2 (16–36%)	26°	NL

2. Results of the research and discussion

The analysis of the experiments presented in the study based on in-cylinder pressure data acquisition. The 200 consecutive engine-working cycles of each combustible mixture and HES collected for the analysis. The impact of HES on combustion properties and combustion duration of the CI engine operating with the RME under fixed injection timing at three engine loads studied.

In-cylinder maximum pressure curves for various hydrogen fractions are provided at the Figure 2. The increase of in-cylinder maximum pressure commenced when HES overstep the 16% at the ML and NL. The trace of in-cylinder maximum pressure at the LL decreased with HES of 19% then does not changed significantly and when HES overstep the 32% of HES pressure began to rise. The in-cylinder pressure decreased during the lean burn of the λ = 3.49–3.92, unless addition of 19–32% HES. However, the main reason of this decrease is the low hydrogen volume fraction, which was far below of the LFL of hydrogen. The hydrogen volume fraction at the HES of 19% was 1.5%, at the 26% HES – 2.25%, at the 32% HES – 3% and all these values were below the LFL of 4% (Table 1). There should be mentioned that with increase of temperature and pressure the flammability limits of the hydrogen-air mixture are changing. The experiments show that limits became wider with increasing temperature (Schroeder & Holtappels, 2004). The linear function of LFL was described in the temperature range up to the actual SOC, which was in the temperature range of 415–435 °C during the experiment performed by author. According to the Schroeder & Holtappels (2004), LFL can be expressed by the formula:

$$LFL = LFL_0 \cdot (1 - K_L \cdot (T - T_0)), \quad (2)$$

where: LFL_0 – LFL at 0 °C, K_L – dependence factor on temperature increase, K_L = 0.000157 K^{-1}, T – designated temperature, T_0 = 273.15 °C.

The LFL at the SOC temperature was 1.5% of hydrogen volume fraction. The LFL decreased by 2.5% starting form 4%. This decrease of LFL do not contribute the SOC of hydrogen as the temperature is still too low (415–435 °C) and not sufficient for autoignition of hydrogen and to assist the intensity of combustion.

However, with increase of pressure up to 50 bar the LFL increasing from 4% to 5.6%. Further, with increase of pressure up to 150 bar no changes has been noticed (Schroeder & Holtappels, 2004; Schroeder, Emonts, Janssen, & Schulze, 2004). Therefore at the moment of the SOC the pressure was 3.98 MPa (39.8 bar) and the LFL was 3.0–3.1% of hydrogen volume fraction. We can conclude that only with HES of 32%, LFL was achieved and hydrogen effectively co-combusted with injected RME. Before that, the lean mixture of air – hydrogen with RME is still flammable but non-coherent, it burns incompletely and does not make positive effect on the combustion intensity and engine performance (Verhelst & Wallner, 2009). The same explanation related to the poor performance of p_{max} with low HES = 16%, rich fuel mixtures at ML (λ = 2.12) and NL (λ = 1.54).

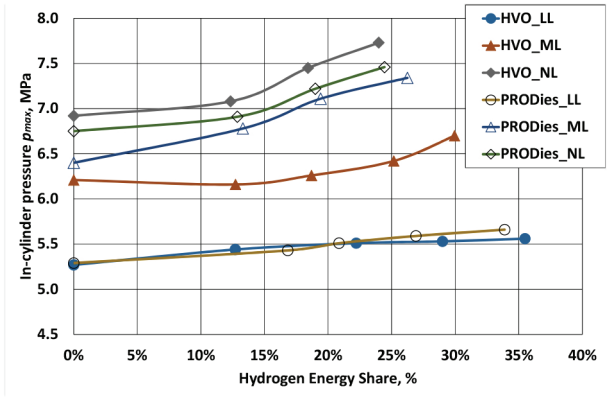

Figure 2. In-cylinder max pressure at Low, Medium and Nominal Loads and HES

In-cylinder pressure curves for RME+$H_2$0%, RME+$H_2$32% at LL and RME+$H_2$30% at ML – NL are provided at the Figure 3 with the position of SOC of corresponding mixtures. The SOC was taken at crank angle at which the curve of the ROHR changes its value from the minus side to plus one. For the accuracy of the evaluation 200 single-cycle in-cylinder pressure diagrams were recorded. Therefore the SOC was averaged over 200 combustion cycles. The position of the SOC was veryfied after AVL simulation (Figure 9). The SOC of sole RME without presence of hydrogen takes place earlier as it can be seen at the Figure 3, because SOI was earlier too (Table 2, test no. 1, 3 and 5).

In-cylinder pressure with sole RME at LL was higher than at operation with hydrogen as it can be seen at the Figure 3. The hydrogen due to the low volume fraction in the combustion chamber not intensified the combustion. The lean hydrogen – air mixture does not support the flame propagation and results in rather low hydrogen combustion efficiency (Saravanan, Nagarajan, & Narayanasamy, 2017). After the boundary of hydrogen volume flammability lower limit was exceeded, with HES of 30% at ML and NL, the combustion became more intensive, especially at the premixed phase and in-cylinder pressure as well as p_{max} increased. The engine operation limits was noticed with RME as the abnormal combustion (knocking) appeared when λ

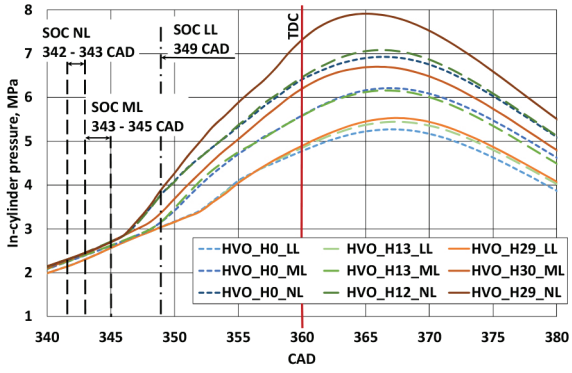

Figure 3. In-cylinder pressure dependence on CAD and position of SOC at Low and Nominal Loads

reached the rich burn rates of 1.44–1.66 (at the NL) and HES more than 36%, as the injection timing fixed.

AVL BOOST (2011) simulation revealed that the hydrogen fraction at the LL do not affects significantly the combustion intensity of the fuel mixture. The lean hydrogen – RME mixture does not support the flame propagation and results the slow increase of the pressure-rise, plotted at the Figure 4. The more significant increase of the pressure-rise because of HES noticed at the NL. The combustion became more intensive at the premixed phase and $dp/d\phi$ increased from 0.256 MPa/deg to 0.304 MPa/deg. The presence of hydrogen do not influenced the pressure-rise at the LL and lean burn with λ = 3.26–3.92. The marginal increase of $dp/d\phi$ was only 4.6% with increase of HES from 19% to 32% influenced mainly by the low volumetric hydrogen fraction, which was insufficient to overcome the lower flammability limit of hydrogen.

Experiments revealed that with the hydrogen – RME mixture operation achieve the higher in-cylinder pressure than a sole RME operation. However, the *ISFC* decreases with increase of HES and at the medium (λ = 1.95–2.15) and nominal loads (λ = 1.44–1.66) has the highest decrease of *ISFC* by 28% in compare to sole RME because of increase of the mass flow rate of hydrogen (Figure 5). Hydrogen due to high flame speed and short quenching distance extends the flammability range of RME – hydrogen mixture, ensure RME combusted completely under especially higher load conditions, which provides reduced *ISFC* (Baltacioglu et al., 2016). The substitution of RME by hydrogen makes positive affect on *ISFC*.

The *ITE* changed during the tests with increase of the HES in the following way: it decreased at the lean burn by 11%, and increased by 11.4% when hydrogen – RME mixture get rich burn at the ML and NL (Figure 6). As it was mentioned before, the presence of the hydrogen affects the combustion intensity only at the rich burn mixture. The lower heating value of the fuel mixture did not change, with increased engine load, and therefore did not make any significant effect on *ITE*. The biggest influence on the *ITE*, was made by increased mass flow rate of the hydrogen as the response to the decreased total fuel mass flow rate and *ISFC* (Figure 5).

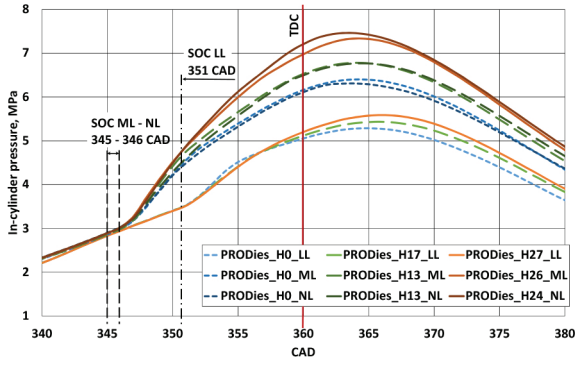

Figure 4. The pressure-rise as the function of CA at the LL and NL with various HES

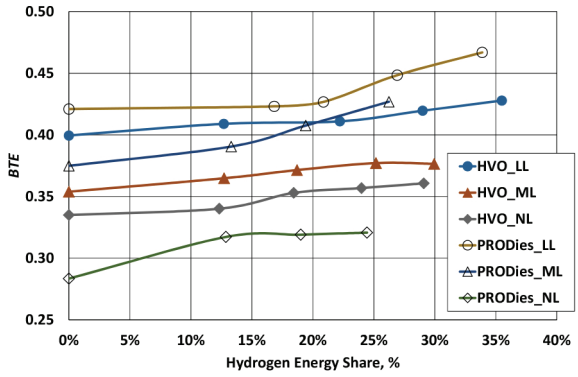

Figure 5. The dependence of ISFC on fuel used, loads and HES

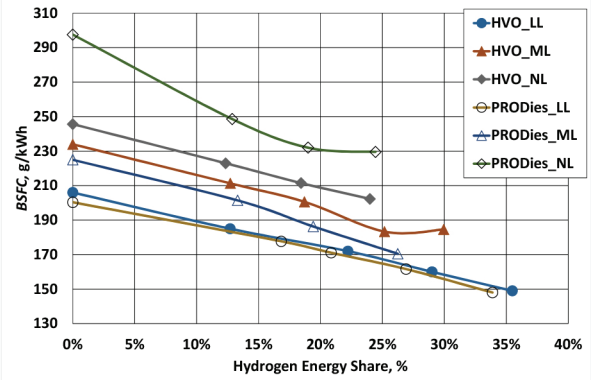

Figure 6. The dependence of *ITE* on fuel used, loads and HES

The increased hydrogen increment rate caused the decrease of C/H ratio and that causes the reduction of CO and CO_2 emission in the exhaust gas as well as reduction of its smokiness as shown at the Figure 8 (Aldhaidhawi et al., 2017; Barrios, Domínguez-Sáez, & Hormigo, 2017; Rocha, Pereira, Nogueira, Belchior, & Tostes, 2016).

The addition of hydrogen up to 15% HES decreased the NO levels at ML and NL, however with the further HES increase of more than 15% NO increased significantly (Figure 7). At the LL the increase of NO is negligible at the whole test range of HES because the lean hydrogen – air mixture does not support the flame propagation and results in low combustion temperature. Senthil Kumar (2003) and Bika et al. (2008) observed the NO_X reduction at the low HES of 5%. This NO reduction is due to the slower combustion caused by a shorter ignition lag that contributes to advanced ignition, which decreases the combustion rate just after start of combustion (Grab-Rogalinski & Szwaja, 2016). The highest increase rate of NO was at the nominal load at the top HES of experiment. However, the increase of HES, led to a reduction of smokiness (Figure 8).

The ROHR as pressure-rise over CA was determined by AVL BOOST simulation software of engine cycles and gas exchanges (AVL BOOST, 2011). The increment of hydrogen fraction generated the step-by step increase of maximum ROHR by 27.1% from 48.76 J/deg to 61.98 J/deg

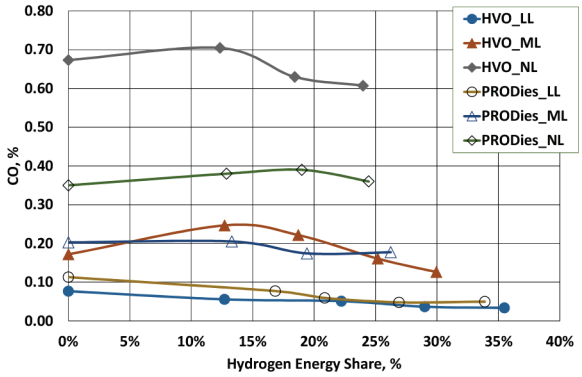

Figure 7. The dependence of NO on the load and HES

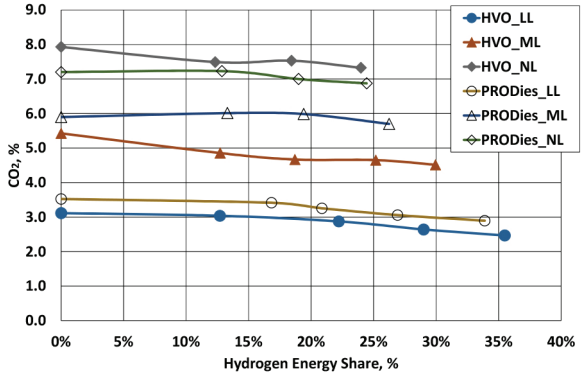

Figure 8. The dependence of smokiness on the load and HES

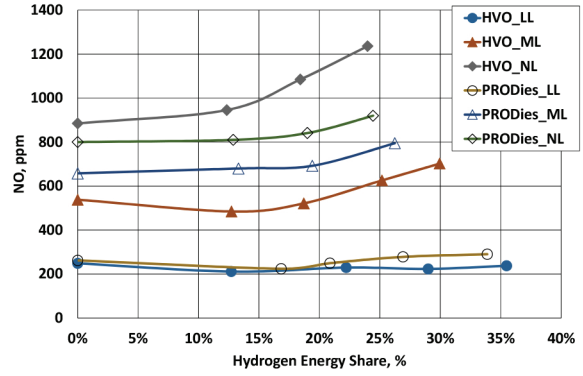

Figure 9. The ROHR history at the LL and NL with various HES

at the low load (Figure 9). At the nominal load, the ROHR maximum value increased from 82.64 J/deg to 104.35 J/deg. The $ROHR_{max}$ increased by 26.3%, slightly lower than at the low load. This result could lead to the contradiction with conclusion made before, that co-combustion of hydrogen with RME mixture at the LL was sluggish and hydrogen makes positive effect on the engine performance only with the LFL of 3.0–3.1% of hydrogen volume fraction. However, in this case most important factor is the lower heating value of the hydrogen – RME mixture. The lower heating value of the fuel mixture did not changed when λ decreased with increase of engine load at the same HES. Therefore ROHR increased by 26.3–27.1% and λ did not make significant effect. However this gain of ROHR determines the increase of NO with λ = 1.44–1.66, from 535 ppm with HES = 16% to 965 ppm with HES of 32% at the NL (Figure 7) and matches well with the test results of other researchers (Barrios et al., 2017; Rocha et al., 2016).

With AVL BOOST of a two-zone combustion model (AVL BOOST, 2011) has been determined the intensity of the ROHR during the working cycle using (Ghojel, 2010) the Wiebe heat release function:

$$\frac{dx}{d\phi} = a\frac{m_v+1}{\phi_C}\left(\frac{\phi}{\phi_C}\right)^{m_v} e^{-a\left(\frac{\phi}{\phi_c}\right)^{m_v+1}}, \quad (3)$$

where: $dx = \frac{dQ}{Q}$; Q – cyclic heat release rate; φ – crank angle from SOC; φ_c – CD; m_v – combustion intensity shape parameter of the Wiebe function; a – efficiency parameter of the Wiebe function. For a CD corresponding to 0–99.9% MFB a = 6.9078 (Yeliana, Cooney, Worm, Michalek, & Naber, 2008).

During tests, the engine operation limit was reached and the abnormal combustion (knocking) appeared when λ reached the rates of 1.44 at the NL and with HES of 36%. The increase of shape parameter m_v was observed at the lean burn LL with HES up to 32% and decrease of shape parameter m_v was observed at the ML – NL with increase of HES to the engine operation limits. In order to find the engine performance parameters including combustion shape parameter m_v and CD, with HES of more than 36%, the numerical simulation AVL BOOST two-zone model software applied.

The simulation was performed with hydrogen fraction of more than the top limits reached during the experiment: 42% at the ML and 36% at the NL, with presumption to get the combustion intensity behavior with extreemely high HES. The hydrogen fractions of 47%, 55%, 64%, 71% were determined for the ML and HES of 42%, 47%, 50%, 62%, 72% for the NL. Also the hydrogen – RME mixture mass flow rates determined and input to the AVL BOOST. The numerical simulation was performed at the same engine speed of 960 rpm, and with decreasing **λ** as the air mass flow rate decreased due to significantly increased hydrogen flow rate. In fact the lower heating value of the fuel mixture reach the value of 73.5 – 74.2 MJ/kg, twice as the lower heating value of sole RME.

The shape parameter m_v of the Wiebe function increased from 0.48 with sole RME to 0.52 with RME+$H_2$32%, due to the low hydrogen combustion efficiency, the intensity moved to the middle of the combustion process when simulated at the LL. Then m_v maintains the decreasing trace to 0.44 with RME+$H_2$80%. This simulation case confirms the conclusion that when the LFL was achieved with RME+$H_2$32%, the hydrogen co-combustion efficiency with RME increased, with increment of the intensity at the beginning of combustion process, which is confirmed by lower m_v.

The combustion intensity shape parameter m_v decreased to 0.34 with increase of HES at the ML for slightly richer combustible mixture with λ = 1.82 and to 0.21 for rich combustible mixture λ = 1.37 at the NL. The increasing hydrogen fraction for rich combustible mixtures has inherent ability to accelerate the laminar flame speed and the intensity of combustion at the beginning. Due to the high premixed combustion rate increased the ROHR (Figure 9).

However, with the HES of 42% at the ML and with HES of 36% at the NL abnormal combustion (knocking) appeared and further increase of HES was undesirable for the engine. The combustion intensity shape parameter m_v, it trend lines at the various HES and knock appearance limit is marked at the Figure 10. The hydrogen volume fraction was within the range of 6.91–7.83 when knocking started. The knock appearance limit could dependent on other engine parameters such as SOI, engine speed, compression ratio, hydrogen supply mode etc.

The CD shortened with increase of HES without any significant ups and downs when simulated (Figure 11). The CD shortened by 29.2% from 72 CAD to 51 CAD at the LL and by 27.8% from 108 CAD to 78 CAD at the NL. The presence of hydrogen contributes to decrease the CD due to the high premixed combustion rate and impact of higher laminar speed of hydrogen flame. Increase of hydrogen fraction also reduces the main combustion duration CA 10–90, which was accelerated by the intensified first combustion phase CA 0–10.

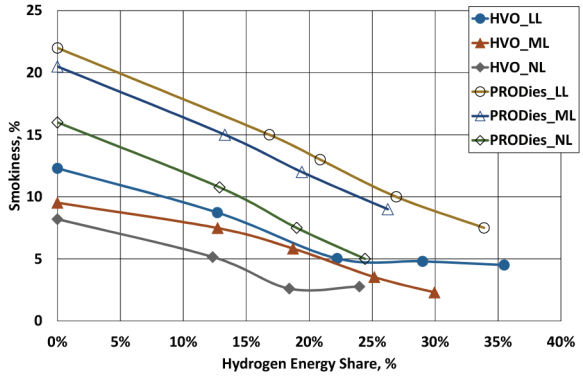

Figure 10. The combustion intensity shape parameter m_v of the Wiebe function and it trend lines at the various HES

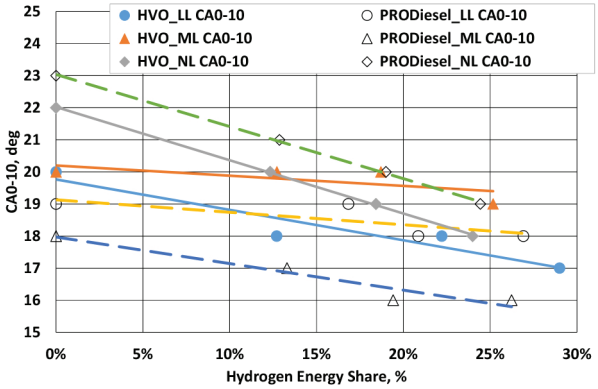

Figure 11. The CD and it trend lines at the various HES

Acknowledgements

This project has received funding from the European Union's Horizon 2020 research and innovation program under the grant agreement No 691232 – Knocky – H2020-MSCA-RISE-2015/H2020-MSCA-RISE-2015. The results of the research obtained by using a simulation tool AVL BOOST, acquired by signing the Cooperation Agreements: AVL Advanced Simulation Technologies – Faculty of Transport Engineering of Vilnius Gediminas Technical University, and AVL Advanced Simulation Technologies – Institute of Thermal Machinery of Czestochowa University of Technology.

Conclusions

The analyses of the test and simulation results revealed the following conclusions:

1. The increase trend of p_{max} was noticed with increase of HES at the all tested loads. However, the lean hydrogen – RME mixture (λ = 3.49–3.92) does not support the flame propagation at the LL due to the too low hydrogen volume fraction, which is insufficient to reach the LFL and results the decrease of p_{max}. The efficient and intensive combustion starts with HES of 32%, corresponding to the LFL = 3.0–3.1% of hydrogen. Poor performance of p_{max} was noticed with low HES = 16% at ML (λ = 2.12) and NL (λ = 1.54) as well, due to the lower hydrogen volume fraction than LFL.
2. The *ISFC* decreases with increase of HES at the all tested loads. The highest decrease of *ISFC* by 28% was noticed at the ML and NL in compare to sole RME because of increased mass flow rate of hydrogen. The substitution of RME by hydrogen makes positive affect on *ISFC*.
3. The *ITE* with increase of the HES decreased at the LL by 11%, and increased by 11.4% when hydrogen – RME mixture get rich burn at the ML and NL. The *ITE* mainly effected by increased mass flow rate of the hydrogen as the response to the decreased *ISFC*.
4. The increased hydrogen increment rate caused the reduction of CO, CO_2 emissions and reduction of smokiness. The increase of HES enhances the temperature, ROHR and contributes the increase of the NO.
5. The HES = 23–26% was found as the optimal percentage with respect to NO emissions. However, *ITE* increases remarkably, while HES exceeds that range.
6. The abnormal combustion appeared with the HES of 42% at the ML and with HES of 36% at the NL. The hydrogen volume fraction was within the range of 6.91–7.83 when knocking started.
7. The combustion intensity was concentrated at the middle of the combustion process until the LFL = 3.0–3.1% of hydrogen was achieved with RME+H32% at the LL. Then concentration of the combustion intensity moved to the beginning of combustion with HES = 39–80%, which was confirmed by lower m_v obtained during the AVL BOOST simulation.

8. The increasing HES < 72% for rich combustible mixtures at the ML and NL accelerates the intensity of combustion at the beginning of the process as it was confirmed by steadlily decreasing combustion shape parameter m_v, obtained in the process of the simulation.

Due to the increased HES, the combustion intensity was located at the premixed phase of combustion (CA 0–10), shortened the ignition lag and supported higher combustion temperature, affecting exhaust emissions. However, abnormal combustion limited the HES at 36–42%, while increase of NO noticed with HES of 25–30%. The abnormal combustion can be avoided by adjustment of injection timing, as it was fixed during experiment. The favorable outcome of hydrogen fraction defined during tests with respect to performance and emission parameters was HES = 23–26%. AVL BOOST simulation enabled to overstep the threshold of abnormal combustion with much higher HES than during experiment. Further increase of HES shortens the ignition lag and combustion was intensified at the very early stage of premixed phase of combustion.

References

Aldhaidhawi, M., Chiriac, R., Bădescu, V., Descombes, G., & Podevin, P. (2017). Investigation on the mixture formation, combustion characteristics and performance of a Diesel engine fueled with Diesel, Biodiesel B20 and hydrogen addition. *International Journal of Hydrogen Energy, 42*, 16793-16807. https://doi.org/10.1016/j.ijhydene.2017.01.222

AVL BOOST v 2011.2. (2011). *AVL BOOST Users Guide*, Graz, Austria (297 p.).

Baltacioglu, M. K., Arat, H. T., Ozcanli, M., & Aydin, K. (2016). Experimental comparison of pure hydrogen and HHO (hydroxy) enriched biodiesel (B10) fuel in a commercial diesel engine. *International Journal of Hydrogen Energy, 41*, 8347-8353. https://doi.org/10.1016/j.ijhydene.2015.11.185

Barreto, L., Makihira, A., & Riahi, K. (2003). The hydrogen economy in the 21st century: a sustainable development scenario. *International Journal of Hydrogen Energy, 28*, 267-284. https://doi.org/10.1016/S0360-3199(02)00074-5

Barrios, C. C., Domínguez-Sáez, A., & Hormigo, D. (2017). Influence of hydrogen addition on combustion characteristics and particle number and size distribution emissions of a TDI diesel engine. *Fuel, 199*, 162-168. https://doi.org/10.1016/j.fuel.2017.02.089

Ghojel, J. I. (2010). Review of the development and applications of the Wiebe function: a tribute to the contribution of Ivan Wiebe to engine research. *International Journal of Engines*, *11*. https://doi.org/10.1243/14680874JER06510

Grab-Rogalinski, K. & Szwaja, S. (2016). The combustion properties analysis of various liquid fuels based on crude oil and renewables. *IOP Conference Series: Materials Science and Engineering*, *148*(1). https://doi.org/10.1088/1757-899X/148/1/012066

Hilbers, T. J., Sprakel, L. M. J., van den Enk, L. B. J., Zaalberg, B., van den Berg, H., & van der Ham, L. G. J. (2015). Green Diesel from Hydrotreated Vegetable Oil Process Design Study. *Chemical Engineering Technology, 38*(4), 651-657. https://doi.org/10.1002/ceat.201400648

Hoekman, S. K., Broch, A., Robbins, C., Ceniceros, E., & Natarajan, M. (2012). Review of biodiesel composition, properties, and specifications. *Renewable and Sustainable Energy Reviews, 16*, 143-169. https://doi.org/10.1016/j.rser.2011.07.143

Jučas, P. (2006). *Chemotologija*. Akademija. LŽŪU Leidybos centras [Chemotology – Academy – LUA Publishing Center] (130 p.).

Knothe, G., Gerpen, J. V., & Krahl, J. (2005). *The biodiesel handbook*. AOCS Press Champaign, Illinois, USA. https://doi.org/10.1201/9781439822357

Knothe, G., & Razon, L. F. (2017). Biodiesel fuels. *Progress in Energy and Combustion Science, 58*(2017), 36–59. https://doi.org/10.1016/j.pecs.2016.08.001

Labeckas, G., Slavinskas, S., & Mažeika, M. (2014). The effect of ethanol–diesel–biodiesel blends on combustion, performance and emissions of a direct injection diesel engine. *Energy Conversion and Management, 79*, 698-720. https://doi.org/10.1016/j.enconman.2013.12.064

Murphy, D. J., & Hall, C. A. S. (2010). Year in review – EROI or energy return on (energy) invested. *Annals of the New York Academy of Sciences*, *1185*(1), 102-118. https://doi.org/10.1111/j.1749-6632.2009.05282

Murray, J., & King, D. (2012). Oil's tipping point has passed. *Nature, 481*(7382), 433-435. https://doi.org/10.1038/481433a

Rapsoila Certificate of Analysis No. 03/17. (2017). *LST EN 14214:2014*. Date of issue: 2017.03.17. SGS Klaipeda Ltd., UAB „Rapsoila".

Raslavičius, L., Keršys, A., Starevičius, M., Sapragonas, J., & Bazaras, Ž. (2014). Biofuels, sustainability and the transport sector in Lithuania. *Renewable and Sustainable Energy Reviews, 32*, 328-346. https://doi.org/10.1016/j.rser.2014.01.019

Rimkus, A., Žaglinskis, J., Rapalis, P., & Skačkauskas, P. (2015). Research on the combustion, energy and emission parameters of diesel fuel and a biomass-to-liquid (BTL) fuel blend in a compression-ignition engine. *Energy Conversion and Management, 106*, 1109-1117. https://doi.org/10.1016/j.enconman.2015.10.047

Rimkus, A., Matijošius, J., Bogdevičius, M., Bereczky, A., & Török, A. (2018). An investigation of the efficiency of using O_2 and H_2 (hydrooxile gas-HHO) gas additives in a CI engine operating on diesel fuel and biodiesel. *Energy, 152*, 640-651. https://doi.org/10.1016/j.energy.2018.03.087

Rocha, H. M. Z., Pereira, R. S., Nogueira, M. F. N., Belchior, C. R. P., & Tostes, M. E. L. (2016). Experimental investigation of hydrogen addition in the intake air of compressed ignition engines running on biodiesel blend. *International Journal of Hydrogen Energy, 12*, 1-10.

Saravanan, N., Nagarajan, G., & Narayanasamy, S. (2017). Experimental investigation on performance and emission characteristics of DI diesel engine with hydrogen fuel. *SAE Technique Paper* 2007-01-17.

Schroeder, V., & Holtappels, K. (2004). Explosion characteristics of hydrogen-air and hydrogen-oxygen mixtures at elevated pressures. *Bundesanstal für Materialforschung und Pruefung (BAM) Research report* – Project SAFEKINEX, contract EVG1-CT-2002-00072.

Schroeder, V., Emonts, B., Janssen, H., & Schulze, H.-P. (2004). Explosion limits of hydrogen/oxygen mixtures at initial pressures up to 200 bar. *Chemical Engineering Technology, 27*(8), 847-851. https://doi.org/10.1002/ceat200403174

Senthil Kumar, M. (2003). Use of hydrogen to enhance the performance of a vegetable oil fueled compression ignition engine. *International Journal of Hydrogen Energy, 28*(10), 11, 43-54.

Silvestrini, A., Monni, S., Pregernig, M., Barbato, A., Dallemand, F. - J., Croci, E., et al. (2010). The role of cities in achieving the EU targets on biofuels for transportation: the cases of Berlin, London, Milan and Helsinki. *Transportation Research Part A: Policy and Practice*, *44*, 403-417. https://doi.org/10.1016/j.tra.2010.03.014

Singh Bika, A., Franklin, L. M., & Kittelson, D. B. (2008). Emissions effects of hydrogen as a supplemental fuel with diesel and biodiesel. *SAE Pap* 2008-01-0648.

Szwaja, S., & Grab-Rogalinski, K. (2009). Hydrogen combustion in a compression ignition diesel engine. *International Journal of Hydrogen Energy*, *34*, 4413-4421. https://doi.org/10.1016/j.ijhydene.2009.03.020

Verhelst, S., & Wallner, T. (2009). Hydrogen-fueled internal combustion engines. Science Direct: *Progress in Energy and Combustion Science, 35*, 490-527. https://doi.org/10.1016/j.pecs.2009.08.001

Yeliana, Y., Cooney, C., Worm, J., Michalek, D., & Naber, J. (2008). Wiebe function parameter determination for mass fraction burn calculation in an ethanol-gasoline fuelled SI engine. *Journal of KONES Powertrain and Transport*, *15*(3), 2008.

Zhou, J. H., Cheung, C. S., & Leung, C. W. (2014). Combustion, performance, regulated and unregulated emissions of a diesel engine with hydrogen addition. *Applied Energy, 126*, 1-12. https://doi.org/10.1016/j.apenergy.2014.03.089

SLĖGINIO UŽDEGIMO VARIKLIO ENERGINIŲ, EFEKTYVUMO IR DEGINIŲ EMISIJOS RODIKLIŲ TYRIMAS NAUDOJANT RAPSŲ METILESTERĮ IR VANDENILĮ

A. Rimkus, R. Juknelevičius

Santrauka

Straipsnyje pateikti tyrimo rezultatai, gauti atlikus bandymą vieno cilindro slėginio uždegimo variklyje su biodegalais – rapsų metilesteriu (RME) ir vandeniliu. Biodegalai įpurškiami akumuliatorine įpurškimo sistema „Common rail“. Šio tyrimo tikslas – ištirti, kaip vandenilis veikia biodegalų degimą, variklio veikimą, jo efektyvumą ir deginių susidarymą. Vandenilio energinė dalis degimo mišinyje buvo keičiama nuo 0 iki 44 %. Vandenilis buvo tiekiamas įsiurbimo fazės metu įsiurbimo kanalu į degimo kamerą, kurioje jis, susimaišęs su oru, sudaro homogeninį mišinį. Bandymai buvo atliekami nekeičiant įpurškimo kampo, nustačius optimalų įpurškimo kampą esant žemai, vidutinei ir nominaliai variklio apkrovai. Išnagrinėjus variklio bandymų rezultatus ir sumodeliavus AVL BOOST programa, buvo pastebėta, kad, esant liesam vandenilio ir RME mišiniui, liepsnos plitimas yra lėtas, mišinys dega neveiksmingai. Tačiau riebus degalų mišinys ir padidinta vandenilio energijos dalis užtikrina degimo intensyvumą degimo proceso pradžioje ir sutrumpina uždegimo gaišties trukmę. AVL BOOST modeliavimas, atliktas plačiu vandenilio energijos dalies diapazonu (16–80 %), patvirtino teiginį, kad degimas tampa intensyvesnis degimo pradžioje dėl padidinto vandenilio kiekio. Didinant vandenilio kiekį, buvo pastebėta, kad išmetamosiose dujose sumažėjo CO, CO_2 ir kietųjų dalelių, tačiau padidėjo NO koncentracija.

Reikšminiai žodžiai: vandenilis, RME, dyzelinas, slėginio uždegimo variklis, degimo procesas, deginių emisija, detonacija.

Notations

Variables and functions
$dp/d\varphi$ – pressure-rise;
m_v – combustion intensity shape parameter;
p – in-cylinder pressure;
p_{max} – in-cylinder maximum pressure;
φ – injection timing;
λ – air-fuel ratio;

Abbreviations
ATDC – after top dead center;
BTDC – before top dead center;
BSFC – Brake Specific Fuel Consumption;
CA – crank angle;
CAD – crank angle degree;
CA 0–10 – initial combustion duration measured by CAD and determined by positions from SOC to 10% MFB;
CA 10–90 – main combustion duration measured by CAD and determined by positions from 10% MFB to 90% MFB;
CD – combustion duration;
C/H – carbon to hydrogen ratio;
CI – compression ignition;
CO – carbon monoxide;
CO_2 – carbon dioxide;
CN – cetane number;
DF – diesel fuel;
FAME – Fatty Acid Methyl Esther;
HHO – hydrooxile gas;
HES – hydrogen energy share;
H0 – HES = 0%;
H16 – HES = 16%;
IMEP – indicated mean effective pressure;
ISFC – indicated specific fuel consumption;
ITE – indicated thermal efficiency;
LFL – lower flammability limit;
LL – low load;
MFB – mass fraction burned;
ML – medium load;
NO – nitrogen oxide;
NL – nominal load;
NTP – Normal Temperature and Pressure is defined as conditions at 20°C and 1 atm (101 325 Pa);
RME – Rapeseed Methyl Esther;
RME+$H_2$0% – RME – hydrogen mixture with HES = 0%;
RME+$H_2$16% – RME – hydrogen mixture with HES = 16%;
ROHR – rate of heat release;
SOC – start of combustion;
SOI – start of injection;
STP – Standard Temperature and Pressure is defined as conditions at 0°C and 1 bar (100 000 Pa);
THC – total unburned hydrocarbon.